

This discussion paper is/has been under review for the journal Atmospheric Measurement Techniques (AMT). Please refer to the corresponding final paper in AMT if available.

Field test of available methods to measure remotely SO₂ and NO_x emissions from ships

J. M. Balzani Lööv¹, B. Alföldy¹, J. Beecken², N. Berg², A. J. C. Berkhout⁴, J. Duyzer³, L. F. L. Gast⁴, J. Hjorth¹, J.-P. Jalkanen⁵, F. Lagler¹, J. Mellqvist², F. Prata⁶, G. R. van der Hoff⁴, H. Westrate³, D. P. J. Swart⁴, and A. Borowiak¹

¹European Commission, Joint Research Centre (JRC), Ispra, Italy

²Chalmers University of Technology (CHA), Göteborg, Sweden

³the Netherlands Organization for Applied Scientific Research (TNO), Delft, the Netherlands

⁴National Institute for Public Health and Environment (RIVM), Bilthoven, the Netherlands

⁵Finnish Meteorological Institute (FMI), Helsinki, Finland

⁶Norwegian Institute for Air Research (NILU), Kjeller, Norway

Received: 28 June 2013 – Accepted: 7 October 2013 – Published: 14 November 2013

Correspondence to: J. Hjorth (jens.hjorth@jrc.ec.europa.eu)

Published by Copernicus Publications on behalf of the European Geosciences Union.

Field test of available methods to measure remotely SO_x and NO_x

J. M. Balzani Lööv et al.

Title Page

Abstract

Introduction

Conclusions

References

Tables

Figures

⏪

⏩

◀

▶

Back

Close

Full Screen / Esc

Printer-friendly Version

Interactive Discussion

Abstract

Methods for the determination of ship fuel sulphur content and NO_x emission factors from remote measurements have been compared in the harbour of Rotterdam and compared to direct stack emission measurements on the ferry Stena Hollandica. The methods were selected based on a review of the available literature on ship emission measurements. They were either optical (LIDAR, DOAS, UV camera), combined with model based estimates of fuel consumption, or based on the so called “sniffer” principle, where SO₂ or NO_x emission factors are determined from simultaneous measurement of the increase of CO₂ and SO₂ or NO_x concentrations in the plume of the ship compared to the background. The measurements were performed from stations at land, from a boat, and from a helicopter. Mobile measurement platforms were found to have important advantages compared to the landbased ones because they allow to optimize the sampling conditions and to sample from ships on the open sea. Although optical methods can provide reliable results, it was found that at the state of the art, the “sniffer” approach is the most convenient technique for determining both SO₂ and NO_x emission factors remotely. The average random error on the determination of SO₂ emission factors comparing two identical instrumental set-ups was 6%. However, it was found that apparently minor differences in the instrumental characteristics, such as response time, could cause significant differences between the emission factors determined. Direct stack measurements showed that about 14% of the fuel sulphur content was not emitted as SO₂. This was supported by the remote measurements and is in agreement with the results of other field studies.

1 Introduction

Since the beginning of the 20th century, when coal steamers replaced sail ships, the atmospheric impact of ship emissions increased almost continuously. According to Endresen et al. (2007), the global fuel consumption, between 1925 and 1980 increased

AMTD

6, 9735–9782, 2013

Field test of available methods to measure remotely SO_x and NO_x

J. M. Balzani Lööv et al.

Title Page

Abstract

Introduction

Conclusions

References

Tables

Figures

⏪

⏩

◀

▶

Back

Close

Full Screen / Esc

Printer-friendly Version

Interactive Discussion



lower than 0.1 % (m/m) during their stay in the harbour. As an alternative to the use of fuels with low FSC, ships are allowed to use an approved SO₂ abatement system (e.g. scrubbers) to reduce sulphur emissions to meet the regulation limits.

NO_x emissions have to respect certain tiers in order to obtain the required Engine International Air Pollution Prevention (EIAPP) certificate for sailing. The emissions can be reduced through modifications of the engine design or through specific abatement systems (e.g. Selective Catalytic Reduction, Humid Air Motor). The different tiers depend on the construction year of the ship: all the ships built within and after the year 2000 have to respect Tier I; more stringent limits are applied for ships build during and after 2011 (Tier II), and for ships build during and after 2016 and operating inside ECAs Tier III applies. The implementation data for Tier III is presently being renegotiated within IMO. Given the long average lifetime of a ship (typically more than 20 yr) a delay can be expected before it will be possible to observe substantial NO_x reductions.

While for NO_x emissions the regulations are implemented through the periodical release of the EIAPP certificates, the effective implementation regarding SO_x emissions is more complicated. The latter, being dependent on the FSC used at a particular time and location, require effective sampling controls in order to verify the implementation. Because of the important price difference between fuel with low and high FSC, there is an economical advantage in ignoring the regulation. The Signatory States should take enforcement action to vessels under their flag, and additionally to vessels of all flags while in their ports. These checks should be performed during Port State Control (PSC) inspections by every Signatory State. According to the United Nations Convention on the Law of the Sea (UNCLOS, 1982) and the MARPOL code, a ship, whenever not in internal waters (e.g. inside a port), can be boarded only if there are clear grounds to suspect that the ship is not respecting the regulations: the only way to collect *a priori* these proofs is by “remote sensing” techniques. In addition, on international waters it is not possible to board any vessels and instead a complaint to the flagstate has to be made.

Field test of available methods to measure remotely SO_x and NO_x

J. M. Balzani Lööv et al.

Title Page

Abstract

Introduction

Conclusions

References

Tables

Figures



Back

Close

Full Screen / Esc

Printer-friendly Version

Interactive Discussion



(DOAS) used by CHA, Light Detection And Ranging (LIDAR) used by the National Institute for Public Health and Environment (RIVM), and the Ultraviolet Camera (UV-CAM) technique used by the Norwegian Institute for Air Research (NILU).

Measurements were performed in the period between 17 and 30 of September 2009.

5 An overview of the dates in which each instrument was running is given in Table 1. In order to get additional information on the performance of the remote sensing methods the stack emissions of the Stena Hollandica ferry were measured between the 22 and 30 September. The STEAM model from the Finnish Meteorological Institute (FMI) was used to calculate fuel consumption.

10 Further details about the “sniffer” measurements performed during this campaign and their results are given by Alföldy et al. (2013).

2.1 Measurement locations and meteorological conditions

The measurements were performed in Hoek van Holland (the Netherlands) at the entrance of the Port of Rotterdam. This location was considered the most suitable because of the high volume of daily traffic, the Port of Rotterdam being the busiest harbour in Europe. Furthermore, facing the North Sea, it allowed testing the instruments in meteorological and light conditions characteristic of the European ECA zones (the Baltic and the North Sea). Within these ECAs, at the time of the measurement campaign, the FSC limit was 1.5 % (m/m).

20 Figure 1 shows the positions of the instruments during the campaign. Depending on the terminal they are heading for or coming from, the ships have to follow one of the two main channels: the Nieuwe Waterweg or the Calandkanaal. Mainly two sites were used for the measurements (Hoek van Holland and Landtong) to sample the largest possible number of ships transiting in the Nieuwe Waterweg; the choice of site was depending on the wind direction. A third site (Maasvlakte), located close to the outer entrance of the channel, was used only once. On selected days it was possible to install the instruments on-board moving platforms: a fire brigade vessel of the Rotterdam

Field test of available methods to measure remotely SO_x and NO_x

J. M. Balzani Lööv et al.

Title Page

Abstract

Introduction

Conclusions

References

Tables

Figures

⏪

⏩

◀

▶

Back

Close

Full Screen / Esc

Printer-friendly Version

Interactive Discussion



Port Authorities and a helicopter. Figure 1 shows also the position of the Stena Lines terminal: during the campaign it was possible to measure the emissions on-board the Stena Hollandica, a roll on/roll off passenger ferry (ROPAX) operated daily between Hoek van Holland (NL) and Harwich (UK).

The fair weather and the strong wind offered reasonable conditions on land for 7 days out of 13 for both optical and “sniffing” methods. Measurements were not successful on the 19 and 24 September because of the wind direction being almost parallel to the channel and on the 27th because of gusty winds. Measurements were only partially successful on the 23rd and 29th because of almost parallel wind and on the 26th because of very low wind speed.

2.2 Identification of target vessels

In order to assess the compliance of a ship with the existing fuel regulations, it has to be unambiguously identified. The majority of the merchant ships of 100 GT and above (there are exemptions for e.g. fishing vessels) are identified by a unique IMO ship identification number made of the three letters “IMO” followed by the seven-digit number assigned to all ships by IHS Fairplay when constructed. When the IMO number is not clearly visible, it is possible to have a precise identification through the Automatic Identification System (AIS, obligatory on ships above 300 GT). AIS is an automated tracking system used on ships and by Vessel Traffic Services (VTS) for identifying and locating vessels by electronically exchanging data with other nearby ships and VTS stations. These data can be recorded by an AIS receiver, or it can be obtained from a public website at the time of the measurements (e.g. <http://www.marinetraffic.com>), or it can be made available by the coastguards of the respective member states.

The identification of the plume of a particular vessel is based on the apparent wind, the resultant of the created wind from the speed of the boat, and the true wind. The ship exhaust follows the apparent wind as shown in Fig. 2 (Berg et al., 2012). Direction as well as speed of the apparent wind can be significantly changed by changing the ship speed, in the figure the apparent wind changes by 90° for a ship with opposite

Field test of available methods to measure remotely SO_x and NO_x

J. M. Balzani Lööv et al.

Title Page

Abstract

Introduction

Conclusions

References

Tables

Figures



Back

Close

Full Screen / Esc

Printer-friendly Version

Interactive Discussion



orientation. This can result in overlapping of plumes of two ships with very different positions. For this reason measurement of wind speed and direction is essential for ship identification.

2.3 Measurement platforms

5 Fixed land based monitoring stations offer the advantage of lower costs and the possibility of being fully automatic. However the probability of sampling the ship plume is related to its transport towards the measurement point (function of the wind direction), and the mixing state of the air parcel. Using a mobile (ground-, water-, or airborne) station it is possible to maximize the sampling probability by positioning the instrument
10 downwind of the emission source and by moving closer to it. During the SIRENAS-R campaign, the CHA “sniffing” system was tested on ground-, water- and airborne platforms. Installing the instruments on a ship allows targeting particular ships approaching them from the downwind direction. However, it is not possible to perform measurements in shallow wind conditions when the plume upraises quickly above 50 m, not allowing
15 measurements at sea level. Airborne measurements, despite the high costs for rental of helicopters/planes, allow for fast checks on target ships also at tens of miles from the coast and considering the large area that can be covered this makes the measurements cost effective, compared to other options. While the helicopter is easier to manoeuvre, allowing to measure plumes closer to the sea surface and to do repeated
20 measurements, the airplane allows to reach locations far off the coast more rapidly and the hourly cost is also considerably less for the latter platform.

During the SIRENAS-R campaign mostly land based measurement platforms were used that were chosen according to the wind direction. In addition, one day ship based and five days helicopter based mobile platforms were used.

Field test of available methods to measure remotely SO_x and NO_x

J. M. Balzani Lööv et al.

Title Page

Abstract

Introduction

Conclusions

References

Tables

Figures

⏪

⏩

◀

▶

Back

Close

Full Screen / Esc

Printer-friendly Version

Interactive Discussion



2.4 Sniffing systems

So-called “sniffer systems” have been used by JRC, CHA and TNO in order to measure the SO₂, CO₂, NO and NO_x concentrations of the ship plumes, which are transported from the ship exhaust to the mobile laboratories on the shore site.

The sniffer systems were composed of three commercial air quality analysers, one for the measurement of SO₂, one for the measurement of NO and NO_x, and another one for the measurement of CO₂. The JRC set up comprised two NO/NO_x analysers, to improve the response time by avoiding switching between NO and NO_x measurement.

The measurement of sulphur dioxide is based on fluorescence spectroscopy principles. SO₂ exhibits a strong ultraviolet absorption spectrum between 200 and 240 nm, when it absorbs UV from this, emissions of photons occur (300–400 nm). The amount of fluorescence emitted is directly proportional to the SO₂ concentration. The instruments used were all from Thermo Electron, model 43i-TLE in the case of CHA, 43A in the case of TNO and 43C-TL in the case of the JRC. The instruments are equipped with a hydrocarbon kicker to prevent inaccuracies due to interferences from aromatic VOCs. In order to increase the flow to reduce the response time, CHA had removed this hydrocarbon kicker; the increased flow (5 L min⁻¹) allowed to reach a response time (t₉₀) of 2 s, which is needed for the flight operation (Mellqvist and Berg, 2010). T₉₀ is defined as the time it takes to reach 90 % of the stable response after a step change in the sample concentration (EN 14 626). The critical orifice inside the JRC instrument has been modified to a larger diameter because this was found to reduce the response time. In order to reduce the response time to a t₉₀ of about 15 s the time constant of the JRC instrument was set to 1 s. The TNO instrument had a response time of 19 s and had the hydrocarbon kicker inserted. For calibration, a reference gas mixture of about 100 ppbv SO₂ in synthetic air and SO₂ free synthetic air for the zero calibration have been used.

The NO-NO_x measurements were performed by Thermo Scientific 42C instruments in the case of the JRC while CHA used a Thermo 42i-TL instrument and TNO used

AMTD

6, 9735–9782, 2013

Field test of available methods to measure remotely SO_x and NO_x

J. M. Balzani Lööv et al.

Title Page

Abstract

Introduction

Conclusions

References

Tables

Figures

⏪

⏩

◀

▶

Back

Close

Full Screen / Esc

Printer-friendly Version

Interactive Discussion

Field test of available methods to measure remotely SO_x and NO_x

J. M. Balzani Lööv et al.

Title Page

Abstract

Introduction

Conclusions

References

Tables

Figures

◀

▶

◀

▶

Back

Close

Full Screen / Esc

Printer-friendly Version

Interactive Discussion



Sampling, maintenance and operation of the instruments are performed according to standard operating procedures based on the EN standards (EN 14211 for NO_x and EN 14212 for SO₂), the “Guide to Meteorological Instruments and Methods of Observation” (WMO, 2008) and the recommendations in the manuals of the different instruments.

Whenever a ship plume arrived to the sniffing system, the peak areas of the SO₂ and CO₂ measurements were determined and the background was subtracted. For the land-based instruments, the duration of a peak (i.e. the time period where the plume was intercepted by the instruments) was typically in the range between 30 and 90 s.

Applying the equations below, the sulphur content can be calculated.

Considering the molecular weight of carbon (12 g mol⁻¹) and sulphur (32 g mol⁻¹); and the carbon mass percent in the fuel (87 ± 1.5 %; Cooper et al., 2005; EPA, 2010), the sulphur mass percent of the fuel can be expressed as:

$$\text{SFC}(\%m/m) = \frac{[\text{SO}_2](\text{ppb})32}{[\text{CO}_2](\text{ppb})12} \cdot 0.87 \cdot 100 = \text{SFC}(\%m/m) = \frac{[\text{SO}_2](\text{ppb})}{[\text{CO}_2](\text{ppb})} \cdot 0.232$$

where c is the measured net volume mixing ratio (over the background) of the components.

The fuel mass weighted NO_x emission rate can be calculated from the NO_x/CO₂ ratio. Considering the molecular weight of carbon (12 g mol⁻¹), nitrogen (14 g mol⁻¹) and oxygen (16 g mol⁻¹) and the carbon mass percent in the fuel (87 % (m/m) ± 1.5 % (m/m)) (Cooper, 2003), the fuel mass weighted NO_x emission can be calculated (in g kg⁻¹). This value can be converted to engine power weighted NO_x emission applying the typical specific fuel efficiency that varies from 160 g kWh⁻¹ to 210 g kWh⁻¹ depending on the engine type (Cooper, 2005; Dalsoren et al., 2009).

The engine power weighted NO_x emission rate (E/P) can be formulated:

$$\frac{E}{P} \left[\frac{g}{\text{kWh}} \right] = \frac{c(\text{NO}_x)[\text{ppb}]}{c(\text{CO}_2)[\text{ppb}]} \cdot \frac{46}{12} \cdot 0.87 \cdot e \left[\frac{g}{\text{kWh}} \right] = 3.33 \cdot \frac{c(\text{NO}_x)[\text{ppb}]}{c(\text{CO}_2)[\text{ppb}]} \cdot e \left[\frac{g}{\text{kWh}} \right],$$

where c is the measured net volume mixing ratio of the components, while e [$g kWh^{-1}$] is the fuel efficiency.

Consideration and subtraction of the background is also necessary for NO and NO_x; this can be accomplished in the same way as described for the calculation of the sulphur content. In the case of NO_x, the background, which is subtracted before calculation of the emission factors, can be influenced by interference from other oxidized nitrogen species as mentioned above. However, these species are generally not emitted directly from the combustions source in significant amounts but formed by (photo-) chemical processes taking place in the atmosphere so the measurements of NO_x emissions are unlikely to be influenced by interfering oxidized nitrogen species. At the time scale of a few minutes for the residence time of the NO_x emitted from a ship in the atmosphere before it is measured by the NO_x-analyser, the conversion of NO and NO₂ to other oxidized nitrogen species such as PAN or HNO₃ can be considered as being negligible.

2.5 Optical systems

Optical systems, when the wind field is known, allow to measure emission rates for several substances. During the SIRENAS-R campaign, three different optical instruments were used to determine the SO₂ emission rates of several ships: DOAS, LIDAR, and UV-CAM. The DOAS unit used was also able to measure NO₂ emission rates.

2.5.1 DOAS

The DOAS technique (Platt et al., 1979) is widely used for many applications. During the campaign a DOAS unit was operated by CHA from a Dauphin helicopter (Berg et al., 2012).

The system consists of a UV/visible spectrometer operating either around the 300 nm region or around 430 nm for measuring SO₂ and NO₂, respectively. The spectrometer is connected to an optical telescope via a liquid guide fiber.

Field test of available methods to measure remotely SO_x and NO_x

J. M. Balzani Lööv et al.

Title Page

Abstract

Introduction

Conclusions

References

Tables

Figures

⏪

⏩

◀

▶

Back

Close

Full Screen / Esc

Printer-friendly Version

Interactive Discussion



Field test of available methods to measure remotely SO_x and NO_x

J. M. Balzani Lööv et al.

Title Page

Abstract

Introduction

Conclusions

References

Tables

Figures

◀

▶

◀

▶

Back

Close

Full Screen / Esc

Printer-friendly Version

Interactive Discussion

During land/ship based measurements, the telescope points upwards, intercepting above it the plume of a ship passing by. During air based measurements, the telescope point downwards with 30° angle from the horizon. In this case, since the measurements are made by intersecting the plume perpendicularly to the aircraft heading with the telescope looking on the side of the air platform, the plume is intersected twice.

From the measurement of the spectra, the integrated column of the gas across the plume can be derived, and then recalculated to an absolute emission in kg/s by multiplication with the wind speed. An upper limit to the overall uncertainty has been roughly estimated as 30–45 % while the repeatability was about 20 % during sequential measurements (Berg et al., 2012).

2.5.2 LIDAR

The LIDAR technique is an active optical method where a short laser pulse is sent into the atmosphere. Part of the laser light is scattered back towards the instrument, this light is collected and analysed. The time delay between the emission of the light and its return to the instrument determines the distance to the source of the scattering. A Differential Absorption LIDAR (DIAL) is capable of measuring the concentration of a gas in the atmosphere. It does so by sending out pulses of two or more different wavelengths, chosen so that one wavelength is absorbed stronger by the gas to be measured than the other(s). The distance information along the path of the laser beam is still available, so the instrument determines the concentration at a known place in the atmosphere.

The RIVM mobile LIDAR system sends out laser pulses at 300 094 nm that are absorbed by SO₂ and pulses at 299 752 nm that are not absorbed. The pulses at the two wavelengths are sent out alternately; a total of 30 pulses are sent out each second. Usually, 200 pulses are averaged for a single concentration measurement. The system can scan through the plume allowing to retrieve a bi-dimensional concentration distribution. The optimal measuring conditions occur when it is possible to scan per-

pendicularly to the wind direction. The ship emissions, in g s^{-1} , are given by the product of the wind profile and the concentration profile.

The instrument was designed and built by RIVM. It is extensively described in Volten et al. (2009) and Berkhout et al. (2012). The standard deviation for individual measurements was calculated by Berkhout et al. (2012) as 38 %. In most of the cases it is possible to carry out repeated scans of the same plume. In this case the standard deviation for the average of four scans is 19 %.

2.5.3 UV-CAM

A new approach based on UV imaging has been tested by the Norwegian NILU institute (Prata et al., 2008). The SO_2 imaging camera (UVGasCam) exploits a strong absorption feature of the SO_2 molecule in the UV region (between 280–320 nm) and is composed by a highly sensitive (between 280–320 nm) CCD array (1344×1024 pixels) manufactured by Hamamatsu Photonics and a UV transparent lens objective.

The SO_2 molecules, being in the field-of-view of the camera, causes attenuation of the recorded light intensity. By calibrating the camera using gas cells containing known amounts of SO_2 , the recorded light intensity can be related directly to the path concentration. Because the camera can sample rapidly (several images per second), features in the images can be tracked and the “in plume” wind speed and gas flux can be derived. The compact size of the instrument, the relatively low costs and the easiness of operation would make the instrument potentially attractive for routine monitoring of ship emissions of SO_2 . So far, the data evaluation and treatment is done manually and requires lots of experience and expertise of the operator.

The technique was previously tested in several cases by volcano measurements (Bluth et al., 2007).

AMTD

6, 9735–9782, 2013

Field test of available methods to measure remotely SO_x and NO_x

J. M. Balzani Lööv et al.

Title Page

Abstract

Introduction

Conclusions

References

Tables

Figures

⏪

⏩

◀

▶

Back

Close

Full Screen / Esc

Printer-friendly Version

Interactive Discussion



2.6 Emission model

An alternative to direct emission measurement is the possibility to model the fuel consumption and the associated emissions knowing the main ship information, the speed, and the meteorological data. This is possible using for example the model STEAM (Ship Traffic Emission Assessment Model), developed by FMI (Jalkanen et al., 2009). The modelling work combines vessel water resistance calculations, technical information on ship properties, and fuel consuming systems with activity data from the Automatic Identification System (AIS). If a vessel cannot be identified at all, it is assumed to be a small vessel. The program uses engine rpm (revolutions per minute) data to assign NO_x emission factors, which are based on the IMO Tier I emissions factors (IMO, 1998). Sulphur emission factors are based on the fuel sulphur content and predicted instantaneous fuel consumption of main and auxiliary engines. During the SIRENAS campaign, it was possible to compare the fuel consumption registered on board of Stena Hollandica with the modelled data which showed an agreement within 10% when the ship was travelling at the designed speed. There is a recent update of STEAM (Jalkanen et al., 2012), which facilitates studies of CO and PM, which were not included in the model version used in the SIRENAS work.

2.7 Stena Hollandica on-board stack measurements

In order to gain detailed information on real ship emissions, measurements have been performed on-board of the ship Stena Hollandica. SO₂ and O₂ were measured by a Fisher Rosemount multiple component analyser, GE 2418, based on IR absorption and a paramagnetic sensor, respectively. Another multiple component analyser (Fisher Rosemount 2419) measured NO, CO₂ and CO from their IR absorption, NO₂ from UV absorption and, again, O₂ by a paramagnetic sensor. Analysers were connected by a 10 m heated line at 180 °C, 6 mm inner diameter (PTFE coated) to a stainless steel probe with glass wool particle filter (in-stack). The sampled gas was conditioned using a portable gas cooler with membrane-gas pump. A critical point was to measure the

Field test of available methods to measure remotely SO_x and NO_x

J. M. Balzani Lööv et al.

Title Page

Abstract

Introduction

Conclusions

References

Tables

Figures

◀

▶

◀

▶

Back

Close

Full Screen / Esc

Printer-friendly Version

Interactive Discussion



Field test of available methods to measure remotely SO_x and NO_x

J. M. Balzani Lööv et al.

Title Page

Abstract

Introduction

Conclusions

References

Tables

Figures

⏪

⏩

◀

▶

Back

Close

Full Screen / Esc

Printer-friendly Version

Interactive Discussion

flow of the exhaust gases. Unfortunately, the absence of sufficiently long sections of the exhaust pipes (more than 5 m in this case) did not allow a precise measurement of the flow and therefore calculations based on fuel consumption data have been used instead. The fuel consumption data have been collected directly from the ship computers together with the GPS information. Previous stack emission measurements have been reported in several studies (e.g. Petzold et al., 2007; Moldanova et al., 2009).

The ferry has 4 main engines, which are coupled 2 by 2 (Main Engine 1 + 2 and Main Engine 3 + 4). Additionally other 5 auxiliary engines are found, Aux 1, 2, and 3 are usually run on Heavy Fuel Oil (HFO), while Aux 4 and 5 run on Marine Diesel Oil (MDO). Aux 4 and 5 are mainly operated only during departure and arrival (close to the land measurement location during SIRENAS-R) for the ship thrusters. It was possible to perform measurements only on one stack at a time. This implies that the total emissions had to be calculated scaling the measured engines with the fuel consumption charts collected on board. Also the total flow had to be calculated similarly because it was not been possible to have a connection to the main stack for the flow meter. Unfortunately, the fuel consumption of auxiliary engines 4 and 5 were not recorded continuously. The consumption of MDO was only 7.3% of the total fuel consumption during the period of the measurements; however, the share of MDO is likely to be higher during the manoeuvring phase when leaving and entering the harbour.

A further uncertainty source has been added because it was not possible to have a digital file of the fuel consumption readings. The only way to obtain these was to print screens manually every few hours. The average deviation between the integrated fuel consumption readings and the actual fuel consumption on each leg according to the ships' computer was 8%. We estimate that the uncertainty on the fuel consumption readings on the open sea is approximately 10%, higher during manoeuvring.

The use of the fuel consumption plot and the stack measurements allowed retrieving emissions plots, not including MDO consumption, for several journeys of Stena Hollandica.

3 Field comparison

During the campaign it was possible to measure the vessels using different techniques at the same time. As Table 2 shows, while a large number of parallel data was collected for “sniffing” systems, which were continuously operated, only in a few cases this was possible for the optical systems. This happened primarily because DOAS and LIDAR are limited by wind conditions: to be able to measure the plumes, steady wind orthogonal to the ship movement is needed. Furthermore, the two instruments, as shown in Fig. 3, measure the same ship in two different points at a minimum of 1 km distance, with a time delay of 1–2 min. In our case, the fact that the ship was accelerating and decelerating in the channel did not allow for a real comparison of the different systems. This is true also for modelling because the STEAM model (Jalkanen et al., 2009) was not able to model the acceleration or deceleration to predict the emissions. The UV-CAM, although more flexible in terms of ideal wind conditions during the campaign, was still in development and suffered of lack of spectral selectivity and a tendency of overestimating the SO₂ concentration because of interferences.

Better conditions to evaluate the DOAS system were found during the helicopter measurements in the open sea. In this situation, the speed of the ship is constant, allowing also to compare the results to model predictions, and to perform replicated measurements. In two of these occasions, Stena Hollandica was also measured in the open sea.

3.1 Stena Hollandica

On-board stack measurements (SO₂, CO₂, NO_x, CO, O₂) were performed between 22 and 30 September with the goal of gaining additional quantitative information on the ship emissions. The average sulphur content of HFO determined from the stack measurements during the journeys was of (1.2 ± 0.1) % (m/m) if only the precision (one standard deviation) of the measurement devices is taken into account. This value has to be compared with the previous 5 bunker delivery notes (1.39 ± 0.03) % (m/m)

Field test of available methods to measure remotely SO_x and NO_x

J. M. Balzani Lööv et al.

Title Page

Abstract

Introduction

Conclusions

References

Tables

Figures

⏪

⏩

◀

▶

Back

Close

Full Screen / Esc

Printer-friendly Version

Interactive Discussion



values, and the reanalysis of the MARPOL samples (1.40 ± 0.06) % (m/m) measured by the Det Norske Veritas (DNV) laboratory. The MARPOL samples are small portions of the bunkered fuel, which have to be stored in a sealed container in case of Port State Control inspection.

5 A discrepancy between the actual sulphur fuel content and that determined by plume measurements has also been found in several other studies (e.g. Schlager et al., 2008; Eyring et al., 2010; Lack et al., 2011), including a study performed subsequently on Stena Hollandica (Moldanova et al., 2013) and seems thus to be a commonly observed phenomenon. Partially this can be caused by the fact that also SO₃ and sulphuric acid
10 are formed by the combustion of sulphur containing fuels. During emission studies this has been found to account for between 1 and 8 % of the total sulphur content (Moldanova et al., 2009; Agrawal et al., 2008; Lack et al., 2009; Alföldy et al., 2013). During the SIRENAS-R campaign 4.8 % of the measured sulphur was present as particle sulphate (Alföldy et al., 2013) and consequently it cannot fully explain the observed
15 difference. Thus one possibility is that part of the oxidized sulphur is not being measured because it is deposited before the sampling points; in fact, it is known that the acidity of lubrication oil can increase because of sulphur contamination (ABS, 1984). In addition, there is accumulation of material in the boilers of ship engines and this material regularly has to be removed.

20 3.2 Land based measurements

3.2.1 Sniffing instruments

Generally three simultaneous sniffing measurements were undertaken during the SIRENAS-R campaign (JRC upper and lower sampling points; and TNO). The JRC measurement van was equipped with the two sampling points at 5 and 15 m height, in
25 order to test the influence of the sampling height on measurements. On the 17th and the 18th, CHA was also measuring on the same location as the others. On 16 to 21

Field test of available methods to measure remotely SO_x and NO_x

J. M. Balzani Lööv et al.

Title Page

Abstract

Introduction

Conclusions

References

Tables

Figures

◀

▶

◀

▶

Back

Close

Full Screen / Esc

Printer-friendly Version

Interactive Discussion



September, the TNO SO₂ analyzer was not operational due to technical problems, so only the days from the 22nd onwards could be used for the comparison.

The measurements have been compared by orthogonal linear regression, using the software RTOOL_v4.1.7 (Beik, 2011). We have chosen to force the regression lines through zero because the distribution of the measurement points in some cases made the evaluation of a possible bias very uncertain. Each point represents a determination of the FSC of a ship at a certain moment. Further, we found it reasonable to assume that there would not be any relevant systematic deviation of the measurements from (0,0) at zero emissions, and, in fact, the regression analysis did not show significant biases for any of the comparisons. Outliers have been eliminated, applying the criterion that an outlier deviates by more than two standard errors from the regression line.

The JRC upper and lower sampling points were found to give results in excellent agreement (Fig. 4): the regressions coefficients for lower versus the upper sampling point is 1.02 with a standard error of 0.01. Applying a 95 % confidence interval ($t \times$ standard error) this means that the regression coefficient lies in the interval 1.02 ± 0.02 . In the following analyses, the average JRC values have been used for the comparisons with CHA and TNO and the uncertainty ranges given are 95 % confidence intervals.

Due to instrumental problems, the TNO group did not have any SO₂ measurements for the first days of the comparison, so a comparison of the TNO and CHA observations could not be performed. The comparisons between the JRC measurements and those performed by TNO and CHA for the 17th and the 18th on the Landtong are shown in Fig. 4. The regression coefficient for the comparison of JRC with Chalmers is 1.22 ± 0.08 . The difference between the JRC and the TNO measurements is more pronounced: the regression coefficient with confidence interval is 1.64 ± 0.14 . This relatively large error was found to be due to the fact that TNO tended to measure higher values of SO₂ as well as lower values of CO₂, compared to the JRC.

The NO_x concentration was measured only at the lower sampling point by JRC. In addition, TNO was measuring NO_x at the same location. Chalmers measured the

AMTD

6, 9735–9782, 2013

Field test of available methods to measure remotely SO_x and NO_x

J. M. Balzani Lööv et al.

Title Page

Abstract

Introduction

Conclusions

References

Tables

Figures

⏪

⏩

◀

▶

Back

Close

Full Screen / Esc

Printer-friendly Version

Interactive Discussion

species NO on this location during the first measurement day only. Consequently there were only two parallel NO_x measurements during the major period of the campaign. The measured NO_x-to-CO₂ ratios calculated from the measurement data of the two groups is correlated, but systematic differences were observed between them (Fig. 5).

5 The regression coefficient for the plot of TNO vs. JRC measurements is 1.27 ± 0.04 (95 % confidence interval).

The measurement differences above are not well understood and they are not caused by calibration issues, since all instruments used the same calibration gases. Nevertheless, one problem with sniffers measurements on the shore side, especially
10 in a busy harbour such as Rotterdam, lies in the fact that the background of CO₂ and occasionally SO₂ is quite variable, due to influence of for instance parked ships, power stations and the refineries emitting VOCs in addition to SO₂ and NO_x. This makes the baseline correction quite challenging and for instruments with slow response, the interfering background will influence the measurements. It was found, in fact, that the
15 measurement differences showed a day-to-day variability that may be explained with changing meteorological conditions. For instance, during the Landtong measurements on 18 and 19 September, the Stena Hollandica blew into the sniffer systems quite frequently and this had to be compensated for. We have worked to homogenize the baseline correction but it was not possible to correct for the fact that the instruments all
20 had different time responses.

An estimate of the random error is obtained by comparing the two values of FSC obtained by the JRC with sampling at the upper and the lower inlets: these are two independent sets of measurements, however with all details of the experimental set up, apart from the sampling points, being the same, thus we can assume that the
25 differences between the instruments are due to random error. If each of the two setups is seen as an instrument to measure FSC, the uncertainty between the two instruments

AMTD

6, 9735–9782, 2013

Field test of available methods to measure remotely SO_x and NO_x

J. M. Balzani Lööv et al.

Title Page

Abstract

Introduction

Conclusions

References

Tables

Figures

⏪

⏩

◀

▶

Back

Close

Full Screen / Esc

Printer-friendly Version

Interactive Discussion

different from those obtained on the open sea, however, the contribution from the two auxiliary engines running on MDO with lower sulphur content. In the harbour area, these auxiliary engines are likely to give a significant contribution to the overall emissions from the ship.

Also the NO_x emission factors for Stena Hollandica, relative to power generation (kWh) or to fuel combustion (kg fuel), will depend on the contribution from the auxiliary engines that typically have higher rotational speeds and thus lower NO_x emission factors than the main engines (Alfoldy et al., 2013) and, in fact, also the few available “sniffer” measurements of NO_x were below the on-board stack measurement.

3.2.3 Optical instruments

The range of the emissions measured, for the different systems, in Rotterdam, is given in Fig. 6. While the emissions from the different vessels can differ significantly (simply due to the sizes of the ships or the respective acceleration or deceleration while leaving or entering the channel) it appears that the range of measurements is rather homogeneous except for the UV-camera, which shows generally higher values. Measurements with the UV camera have been performed for most of the days, but so far only the results of the 17 September have been analysed for a total of 11 ships. No other optical technique measured such high emission rates, as is apparent from Fig. 6. In addition, the measured emission rates are higher than can be expected from ships of the appropriate type sailing at full power on high-FSC fuel. This leads to the conclusion that the UV camera most likely overestimates the emission rate values.

The distribution of SO_2 emission rates of the ships measured by DOAS and LIDAR is shown in Fig. 7. The figure shows the multimodal distribution of the SO_2 emission rate. The first, most frequented, mode of the emission rates measured by LIDAR has a maximum at 20 kg h^{-1} emission rate, which is in good agreement with the DOAS results. 78 % of the measured ships are included in this mode. The second mode that contains 15 % of the cases has maximum at 70 kg h^{-1} . This value is higher than the second maximum of DOAS results by 17 %. The remaining 7 % of the ships are distributed be-

Field test of available methods to measure remotely SO_x and NO_x

J. M. Balzani Lööv et al.

Title Page

Abstract

Introduction

Conclusions

References

Tables

Figures

⏪

⏩

◀

▶

Back

Close

Full Screen / Esc

Printer-friendly Version

Interactive Discussion



tween 105, 155 and 205 kg h⁻¹ emission rate bins. The corresponding DOAS bins are also at lower emission rates, in addition, the highest emission rate bins are missing at the DOAS measurement.

The differences between SO₂ emission rate distributions given by the LIDAR and DOAS techniques may be due to the different measurement conditions. LIDAR measurements were performed of arriving or leaving ships, during acceleration or deceleration consequently, while DOAS measurements were made on open sea during steady state operation of the ship engines. It is likely, that the first emission rate peak that has same maximum as the DOAS peak contains measurements made on ships with steady state operation condition, while the second, third, fourth and fifth peaks contain the accelerating/decelerating cases.

Comparison of emission rates of a ship measured by LIDAR and DOAS technique is difficult, since there was no common measurement at the same place and same time. The LIDAR was faced to the open sea, looked forward approximately by 1 km, while DOAS looked up vertically from the measurement site. It means that the distance between the two measurements was 1 km and the minimal time delay 1–2 min. Table 3 summarises the three closest measurements by LIDAR and DOAS technique taken on 17 September; Stena Hollandica arriving and leaving and Stena Britannica arriving. The differences between the two techniques are also indicated.

The arrival and leaving of Stena Hollandica were measured three times per case, while Stena Britannica was measured twice. The repeated measurements provide different emission rate values. The standard deviation of the repeated measurements is especially high in the case of Stena Hollandica leaving (43 %). In this case the emission rate increased by a factor of 3.5 in four minutes. This high deviation does not reflect the uncertainty of the method, rather the different conditions of the measurements. Since LIDAR measurements were taken during the launching manoeuvre of the ship, different engine loads can be expected in the time frame of the three measurements which results in different SO₂ emission.

Field test of available methods to measure remotely SO_x and NO_x

J. M. Balzani Lööv et al.

Title Page

Abstract

Introduction

Conclusions

References

Tables

Figures

⏪

⏩

◀

▶

Back

Close

Full Screen / Esc

Printer-friendly Version

Interactive Discussion

Field test of available methods to measure remotely SO_x and NO_x

J. M. Balzani Lööv et al.

Title Page

Abstract

Introduction

Conclusions

References

Tables

Figures

◀

▶

◀

▶

Back

Close

Full Screen / Esc

Printer-friendly Version

Interactive Discussion



Figure 8 shows the three sequential LIDAR scans of the leaving Stena Hollandica. It is clearly seen, how the emission rate increases with the time and the distance from the measurement location. Consequently, the standard deviation of the repeated measurements does not reflect the uncertainties on the measurement technique only but also the changing emission rate., Under these conditions, the comparison with the DOAS technique could not be done.

On the contrary to the DOAS measurement, the UV-CAM can be compared with the LIDAR since both looked into the same direction and the measurements were performed at the same time. As shown in Fig. 9, the two measurements agree only in two cases (Stena Britannica and Hollandica), in the other cases the UV-CAM significantly overestimates the SO₂ emission rate compared to the LIDAR results. The scattering of the UV-CAM measurements can be due to the presence of particles in the ship plumes, which reflect and absorb a significant part of the incoming UV light. A new version of the UV-CAM with a co-aligned spectrometer may allow to distinguish the fraction of absorption related to the particles from the one related to SO₂.

Important contributions to the uncertainty on the LIDAR determination of ship emissions come from uncertainty on the wind speed measurements, meandering of the plume and noise on the echo signal received by the instrument.

3.3 Measurements from mobile platforms

3.3.1 “Sniffing” instruments

The SO₂ emission factors for Stena Hollandica were determined by helicopter borne ‘sniffer’ measurements by CHA using the same system as applied in the harbour (Berg et al., 2010; Mellqvist, 2010). The 25 measurements on 23, 25 and 27 September of SO₂ and CO₂ gave an average calculated FSC of (1.13 ± 0.18) % (m/m), while the 19 measurements of NO and CO₂ gave an average emission factor of (34 ± 4) g (kg fuel)⁻¹ for NO, Noteworthy is, that NO₂ from the helicopter was not measured and this should add about 20 % to the measured NO_x emission factor according to Alföldy et al. (2013).

The values above should be compared to the on board stack measurements of SO₂ and NO_x that yielded (1.2 ± 0.1) % (m/m) FSC and (41 ± 3 g)(kg fuel)⁻¹, respectively. As discussed in Sect. 2.1, the fuel analysis showed higher FSC, i.e. 1,4 % (m/m). Part of this is due to the fact that sulfate in particles was not measured.

3.3.2 DOAS

The SO₂ emission factor for Stena Hollandica was also determined by DOAS measurements from the helicopter combined with modelling of the fuel consumption, using the STEAM model (Jalkanen et al., 2009). A detailed discussion of this comparison can be found in Berg et al. (2012). The comparison showed differences of (-30 ± 14) % and (-41 ± 11) %, respectively, between the measurements and the certified fuel sulphur content for two days, with equal measurement precision of about 20 %. The agreement with the on-board stack measurements, 14 % below the certified value, is obviously somewhat better. Main contributions to the uncertainties on the DOAS measurements stem from the evaluation of the optical path of the ocean scattered light due to waves, and direct and multiple scattering in the exhaust plume. Rough estimates of these sources have been accounted for in the total uncertainty, which is estimated to be 30–45 % (Berg et al., 2012).

Stena Hollandica was measured outside the channel with the UV-DOAS installed on a helicopter. The result shows a good agreement with the stack measurements performed on-board Stena Hollandica with only a 5 % difference in one case while in the second case the on-board measurements exceeded the DOAS measurements by more than a factor of two (see Table 4). Figure 10 shows the modelled variation of the SO₂ emission rate for the first two hours of the Stena Hollandica journey from Hoek van Holland to Harwich on 25 September. Measured emission rates determined by onboard stack measurement and DOAS technique are also shown in the figure. The latter was performed from the helicopter when the ship reached the steady state operation. The error bar given by repeated DOAS measurements is also indicated. It can be concluded

AMTD

6, 9735–9782, 2013

Field test of available methods to measure remotely SO_x and NO_x

J. M. Balzani Lööv et al.

Title Page

Abstract

Introduction

Conclusions

References

Tables

Figures

⏪

⏩

◀

▶

Back

Close

Full Screen / Esc

Printer-friendly Version

Interactive Discussion

that the modelled value and the two measurement results agree within the error bar of the DOAS measurement.

The uncertainty budget for the DOAS determinations of ship emissions is discussed by Berg et al. (2012). The largest contributions are related to wind speed, influence of waves and plume width.

Comparison of UV-DOAS measurements provided by helicopter flights with model calculations for other ships and with the sniffer measurements is shown in Fig. 11. Model calculations were made based on the assumption that main engines of the ships use fuel with fixed 1.5 % (m/m) FSC, while the auxiliaries run with 0.5 % (m/m) FSC fuels. The model calculation can be refined, if the fixed fuel sulphur ratio is replaced by the real ones determined by the sniffing measurements. It can be seen that in most of the cases (from Lion to Endeavor) the corrected model results lie within the error bars of the UV-DOAS measurements. This finding validates the method by which the fuel sulphur ratio is calculated from the combination of optical SO₂ emission measurement and fuel consumption modelling.

4 Conclusions

The “sniffer” principle, with the state of the art of measurement techniques, appears to provide the most convenient approach to determination of FSC and NO_x emission factors for ships by remote measurements. The experimental results showed that two instruments operated under identical conditions had a precision in the FSC determination of 0.06 % (m/m).

Visual inspection of the data (Fig. 4) suggests that the absolute values of the residuals are approximately independent of the value of the observation. This means that the relative importance of random errors will increase with decreasing FSC, in our case from 6 % for 1 % (m/m) FSC to 60 % for 0.1 % (m/m) FSC. It was found by the comparison of the three groups, that the regression coefficient of the straight line between the observed values can significantly differ from 1, which implies that apparently minor

Field test of available methods to measure remotely SO_x and NO_x

J. M. Balzani Lööv et al.

Title Page

Abstract

Introduction

Conclusions

References

Tables

Figures

⏪

⏩

◀

▶

Back

Close

Full Screen / Esc

Printer-friendly Version

Interactive Discussion



differences in the instrumental characteristics, particularly in the response times, may have a significant impact on the values of the calculated emission factors.

This relatively high standard deviation for low FSCs is a result of the higher uncertainty on the measurement of lower sulphur concentration, but also the higher uncertainty on measurement of lower CO₂ concentration. In fact, the low sulphur fuel was mainly used by small boats (e.g. port authorities and service boats), with a low fuel consumption. Future regulations of ship emissions will lead to lower FSCs and consequently to higher relative errors on their determination, however, as the CO₂ emissions will not decrease like the sulphur content, the uncertainties are likely to be lower than what appears from the above discussion. In addition, a lower background of SO₂ is likely to improve the detection limit of the sniffer method, as discussed in Sect. 2.2.1.

It was found that also the DOAS and the LIDAR techniques can provide reliable estimates of SO₂ emissions from ships, however, they are influenced by relevant additional error sources because the vertical wind profile is needed for the emission rate calculation. In addition, for compliance control it is necessary to complement these measurements with modelling of fuel consumption in order to calculate FSC and emission factors of NO_x. This is presently being implemented operationally by CHA in a Danish Navajo Piper airplane, combining DOAS and the STEAM method (Beecken et al., 2013; Jalkanen et al., 2009).

The UV camera is the cheapest and easiest optical technique; however, it has proved to be the least reliable method in the tested configuration. It is the consequence of the high particle emission of ships that due to scattering modify the recorded light intensity. After further technical developments, the reliability of the measurement may be improved.

The use of a mobile platform has two important advantages: it can allow to position the measurement devices in a favourable position relative to the ship, in the case of the sniffer technique downwind and close to the stack, which optimizes the precision and accuracy of the measurements. Further, it can allow to measure ship emissions under steady state conditions outside internal waters, which are the most relevant condition

Field test of available methods to measure remotely SO_x and NO_x

J. M. Balzani Lööv et al.

Title Page

Abstract

Introduction

Conclusions

References

Tables

Figures

⏪

⏩

◀

▶

Back

Close

Full Screen / Esc

Printer-friendly Version

Interactive Discussion

Field test of available methods to measure remotely SO_x and NO_x

J. M. Balzani Lööv et al.

Title Page

Abstract

Introduction

Conclusions

References

Tables

Figures

◀

▶

◀

▶

Back

Close

Full Screen / Esc

Printer-friendly Version

Interactive Discussion

- Beecken, J., Mellqvist, J., Salo, K., Ekholm, J., and Jalkanen, J.-P.: Airborne Emission Measurements of SO₂, NO_x and Particles from Individual Ships using Sniffer Technique, submitted, Atmospheric Measurement Techniques, 2013.
- Beijk, R.: RIVM Bilthoven the Netherlands Regressiontool: Multi data analyses tool version 4.1.7 (beta), 2011.
- Beijk, R., Mooibroek, D., van de Kasstelee, J., and Hoogerbrugge, R.: PM10: Equivalence study 2006, RIVM Report 680708002/2008, 2008.
- Berg, N., Mellqvist, J., Beecken, J., and Johansson, J.: Ship Emission Measurements by the Chalmers IGPS System during the Rotterdam campaign 2009, RR Report (Göteborg) No.5, ISSN 1653 333X, 2010.
- Berg, N., Mellqvist, J., Jalkanen, J.-P., and Balzani, J.: Ship emissions of SO₂ and NO₂: DOAS measurements from airborne platforms, Atmos. Meas. Tech., 5, 1085–1098, doi:10.5194/amt-5-1085-2012, 2012.
- Berkhout, A. J. C., Swart, D. P. J., van der Hoff, G. R., and Bergwerff, J. B.: Sulphur dioxide emissions of oceangoing vessels measured remotely with Lidar, RIVM Report 609021119, 2012.
- Bluth, G., Shannon, J., Watson, I., Prata, A., and Realmuto, V.: Development of an ultra-violet digital camera for volcanic SO₂ imaging. J. Volcanol. Geoth. Res., 161, 47–56, 2007.
- Cooper, D. A.: Exhaust emissions from ships at berth, Atmos. Environ. 37, 3817–3830, 2003.
- Cooper, D. A.: HCB, PCB, PCDD and PCDF emissions from ships, Atmos. Environ., 39, 4901–4912, doi:10.1016/j.atmosenv.2005.04.037, 2005.
- Corbett, J. J., Wang, C., Winebrake, J. J., and Green, E.: Allocation and forecasting of global ship emissions. Clean Air Task Force Report, 2007.
- Dalsøren, S. B., Eide, M. S., Endresen, Ø., Mjelde, A., Gravir, G., and Isaksen, I. S. A.: Update on emissions and environmental impacts from the international fleet of ships: the contribution from major ship types and ports, Atmos. Chem. Phys., 9, 2171–2194, doi:10.5194/acp-9-2171-2009, 2009.
- Directive 1999/32/EC, Official Journal of the European Union, L 121, p. 13 of 26.4.1999.
- Directive 2005/33/EC, Official Journal of the European Union, L 191, p. 59 of 22.7.2005.
- Duyzer, J., Hollander, K., Verhagen, H., Weststrate, H., Hensen, A., Kraai, A., and Koos, G.: Assessment of emissions of PM and NO_x of sea going vessels by field measurements. TNO report 2006-A-R0341/B, 2006.

Field test of available methods to measure remotely SO_x and NO_x

J. M. Balzani Lööv et al.

Title Page

Abstract

Introduction

Conclusions

References

Tables

Figures

◀

▶

◀

▶

Back

Close

Full Screen / Esc

Printer-friendly Version

Interactive Discussion

- Kendall, M. G. and Stuart, A.: The Advanced Theory of Statistics, Griffin, London, 1969.
- Lack, D.A., Corbett, J.J., Onasch, T., Lerner, B., Massoli, P., Quinn, P.K., Bates, T.S., Covert, D.S., Coffman, D., Berko Sierau, B., Herndon, S., Allan, J., Baynard, T., Lovejoy, E., Ravishankara, A.R., and Williams, E.: Particulate emissions from commercial shipping: Chemical, physical, and optical properties, *J. Geophys. Res.*, 114, D00F04, doi:10.1029/2008JD011300, 2009.
- Lack, D. A., Cappa, C. D., Langridge, J., Bahreini, R., Buffaloe, G., Brock, C., Cerully, K., Coffman, D., Hayden, K., Holloway, J., Lerner, B., Massoli, P., Li, S.-M., McLaren, R., Middlebrook, A. M., Moore, R., Nenes, A., Nuaaman, I., Onasch, T.B., Peischl, J., Perring, A., Quinn, P.K., Ryerson, T., Schwartz, J.P., Spackman, R., Steven C. Wofsy, S.C., Worsnop, D., Xiang, B., and Williams, E.: Impact of Fuel Quality Regulation and Speed Reductions on Shipping Emissions: Implications for Climate and Air Quality, *Environ. Sci. Technol.*, 45, 9052–9060, doi:10.1021/es2013424, 2011.
- Lloyd's Register of Shipping (LR): Marine Exhaust Emissions Research Programme, Lloyd's Register Engineering Services, UK, London, 1995.
- MARPOL 73/78: International Convention for the Prevention of Pollution From Ships, 1973 as modified by the Protocol of 1978 – Annex VI: Prevention of Air Pollution from Ships, International Maritime Organization (IMO), 1973.
- Mellqvist, J. and Berg, N.: Final report to Vinnova: IDENTIFICATION OF GROSS POLLUTING SHIPS RG Report (Göteborg) No. 4, ISSN 1653 333X, Chalmers University of Technology, 2010.
- Mellqvist, J., Berg, N., and Ohlsson, D.: Remote surveillance of the sulfur content and NO_x emissions of ships, Second international conference on Harbors, Air Quality and Climate Change (HAQCC), Rotterdam, 2008.
- Moldanova, J., Fridell, E., Popovicheva, O., Demirdjian, B., Tishkova, V., Faccinnetto, A., and Focsa, C.: Characterisation of particulate matter and gaseous emissions from a large ship diesel engine, *Atmos. Environ.*, 43, 2632–2641, doi:10.1016/j.atmosenv.2009.02.008, 2009.
- Moldanová, J., Fridell, E., Winnes, H., Holmin-Fridell, S., Boman, J., Jedynska, A., Tishkova, V., Demirdjian, B., Joulie, S., Bladt, H., Ivleva, N. P., and Niessner, R.: Physical and chemical characterisation of PM emissions from two ships operating in European Emission Control Areas, *Atmos. Meas. Tech. Discuss.*, 6, 3931–3982, doi:10.5194/amtd-6-3931-2013, 2013.
- Petzold, A., Hasselbach, J., Lauer, P., Baumann, R., Franke, K., Gurk, C., Schlager, H., and Weingartner, E.: Experimental studies on particle emissions from cruising ship, their char-

Field test of available methods to measure remotely SO_x and NO_x

J. M. Balzani Lööv et al.

Title Page

Abstract

Introduction

Conclusions

References

Tables

Figures

⏪

⏩

◀

▶

Back

Close

Full Screen / Esc

Printer-friendly Version

Interactive Discussion



acteristic properties, transformation and atmospheric lifetime in the marine boundary layer, Atmos. Chem. Phys., 8, 2387–2403, doi:10.5194/acp-8-2387-2008, 2008.

Platt, U., Perner, D., and Pätz, H. W.: Simultaneous Measurement of Atmospheric CH₂O, O₃ and NO₂ by Differential Optical Absorption, J. Geophys. Res., 84, 6329–6335, 1979.

5 Prata, A. J. and Bernardo, C.: Retrieval of SO₂ from a ground-based thermal infrared imaging camera system, NILU internal report, 2008.

Schlager, H., Baumann, R., Lichtenstern, M., Petzold, A., Arnold, F., Speidel, M., Gurk, C., and Fischer, H.: Aircraft-based trace gas measurements in a primary European ship corridor. In: Proceedings of the International Conference on Transport. Atmosphere and Climate (TAC), Oxford, UK, 83–88, 2008.

10 UNCLOS: United Nations Convention on the Law of the Sea, 1982.

WMO: Guide to Meteorological Instruments and Methods of Observation, WMO no. 8, 2008.

Volten, H., Brinksma, E. J., Berkhout, A. J. C., Hains, J., Bergwerff, J. B., Van der Hoff, G. R., Apituley, A., Dirksen, R. J., Calabretta-Jongen, S., and Swart, D. P. J.: NO₂ lidar profile measurements for satellite interpretation and validation, J. Geophys. Res., 114, D24301, doi:10.1029/2009JD012441, 2009.

15

Field test of available methods to measure remotely SO_x and NO_x

J. M. Balzani Lööv et al.

Title Page

Abstract

Introduction

Conclusions

References

Tables

Figures

⏪

⏩

◀

▶

Back

Close

Full Screen / Esc

Printer-friendly Version

Interactive Discussion

Table 1. Overview of the measurements, performed in September 2009 during the SIRENAS-R campaign. The table shows the location of the different research groups and their instruments during the measurement days (1: Hoek van Holland, 2: Landtong, 3: Maasvlakte, S: Fire-brigade Ship, H: Helicopter, O: Onboard Stena Hollandica).

	17	18	19	20	21	22	23	24	25	26	27	28	29	30
JRC Sniffer	2	2	2	2	1	1	1	1	1	1	1	1	1	1
TNO Sniffer*	2	2			1	1	1	1	1	1		1	1	
CHA Sniffer/DOAS	2	S	2		1		H	H	H	H	H		1	
NILU UV-CAM	2	2	2	2	1	1	1	1	1	1	1	1	1	
RIVM LIDAR	2	2			1	1	1	1	1					
Stena Stack						O	O	O	O	O	O	O	O	O

* SO₂ was not measured by TNO before the 22nd.

Field test of available methods to measure remotely SO_x and NO_x

J. M. Balzani Lööv et al.

Title Page

Abstract

Introduction

Conclusions

References

Tables

Figures

⏪

⏩

◀

▶

Back

Close

Full Screen / Esc

Printer-friendly Version

Interactive Discussion

Table 2. Overview of the number of ships measured by different techniques during the SIRENAS-R campaign. Relative errors observed by repeated measurement are indicated in the last column (Repeatability). Note, this value for sniffing technique reflects the repeatability of fuel sulphur ratio, while in the optical cases it indicates only the uncertainty of sulphur emission rate. Uncertainty of fuel sulphur ratio is increased by the uncertainty of fuel consumption that is generally a high value. * The LIDAR measured on 7 days, the UV camera on 12 days, but not all data was available for comparisons. ** UV-CAM shows the lowest difference between the repeated measurements, however, it has an important significant bias compared to the others.

	Number of targeted ships	Number of days (out of 13)	Repeatability
Sniffing	475	10	30 %
LIDAR	45	2*	29 %
UV-CAM	11	1*	** 18 %
DOAS (ground + ship)	11	2	20 %
DOAS (helicopter)	20	3	

Field test of available methods to measure remotely SO_x and NO_x

J. M. Balzani Lööv et al.

Title Page

Abstract

Introduction

Conclusions

References

Tables

Figures

⏪

⏩

◀

▶

Back

Close

Full Screen / Esc

Printer-friendly Version

Interactive Discussion



Table 3. Comparison of SO₂ emission rates in kg/h given by DOAS and LIDAR techniques. In the last column, relative differences are presented (DOAS-LIDAR).

	DOAS	LIDAR	Difference
Stena Hollandica, 08:37		57.60	37 %
Stena Hollandica, 08:39	91.10 ± 11 %	66.96	26 %
Stena Hollandica, 08:41		68.40	25 %
Stena Hollandica, average		64.32 ± 9 %	29 %
Stena Hollandica, 15:02		31.72	72 %
Stena Hollandica, 15:04	114.6 ± 14 %	95.04	17 %
Stena Hollandica, 15:06		109.44	4 %
Stena Hollandica, average		78.73 ± 43 %	31 %
Stena Britannica, 16:15		73.44	−147 %
Stena Britannica, 16:17	29.70 ± 9 %	48.96	−65 %
Stena Britannica, average		61.20 ± 28 %	−106 %

Field test of available methods to measure remotely SO_x and NO_x

J. M. Balzani Lööv et al.

Title Page

Abstract

Introduction

Conclusions

References

Tables

Figures

⏪

⏩

◀

▶

Back

Close

Full Screen / Esc

Printer-friendly Version

Interactive Discussion



Table 4. SO₂ emission rates provided by helicopter based DOAS measurements between 23 and 27 September 2009 and compared to on board measurements.

Ship name	Time	Velocity, kn	Emission rate, kg h ⁻¹	St.Dev. %	On board, kg h ⁻¹
Maeris	24/14:40	17	56	40	
Frank	24/15:15	13	19	35	
Taurine	24/15:33	15	12	4	
Sporades	24/15:40	14	20	12	
Altius	24/16:00	14	18	3	
Maersk Ethien	24/16:03	14	23	17	
Lion	25/10:04	15	37	9	
Sloman	25/10:21	14	25	–	
Cap Callisto	25/10:42	16	56	14	
Hyundai	25/11:05	23	129	13	
Deneb J	25/11:25	18	61	17	
Ginga Tiger	25/11:28	16	65	44	
Maas Viking	25/14:20	22	12	16	
St. Hollandica	25/15:02	19	92	19	97
Endevor	27/10:52	18	25	26	
SKS Tugela	27/11:20	16	61	21	
Gennaro	27/11:40	17	29	33	
Genco	27/12:05	17	34	25	
Maersk Fl.	27/14:32	20	32	17	
Katherina B	27/14:50	12	17	31	
St. Hollandica	27/15:06	22	54	18	119

Field test of available methods to measure remotely SO_x and NO_x

J. M. Balzani Lööv et al.

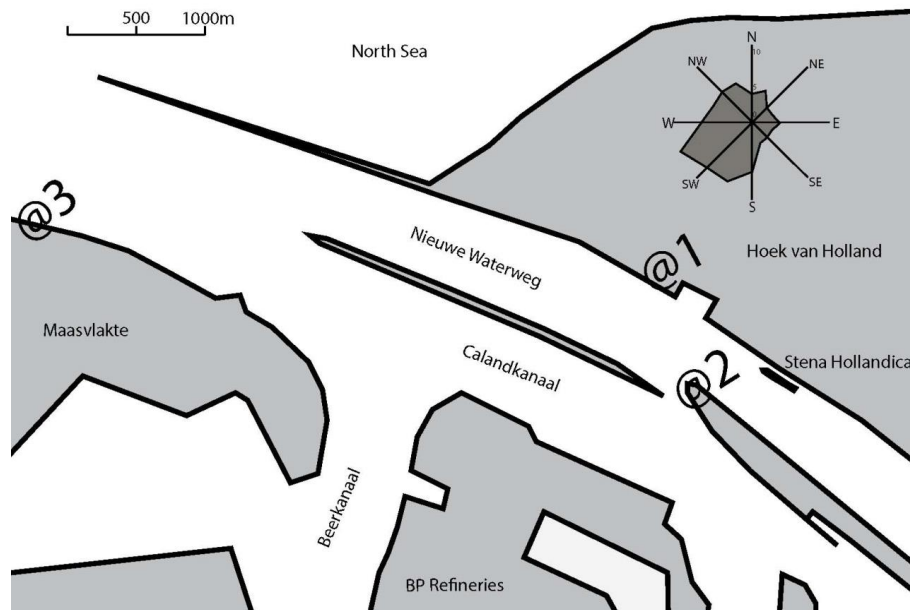


Fig. 1. Scheme of the entrance of the port of Rotterdam and the three measurements points used during the SIRENAS-R campaign (@1 = Hoek van Holland, @2 = Landtong, @3 = Maasvlakte). The berth position of Stena Hollandica and the average wind direction (years 1999–2011) are also indicated.

Title Page

Abstract

Introduction

Conclusions

References

Tables

Figures

⏪

⏩

⏴

⏵

Back

Close

Full Screen / Esc

Printer-friendly Version

Interactive Discussion

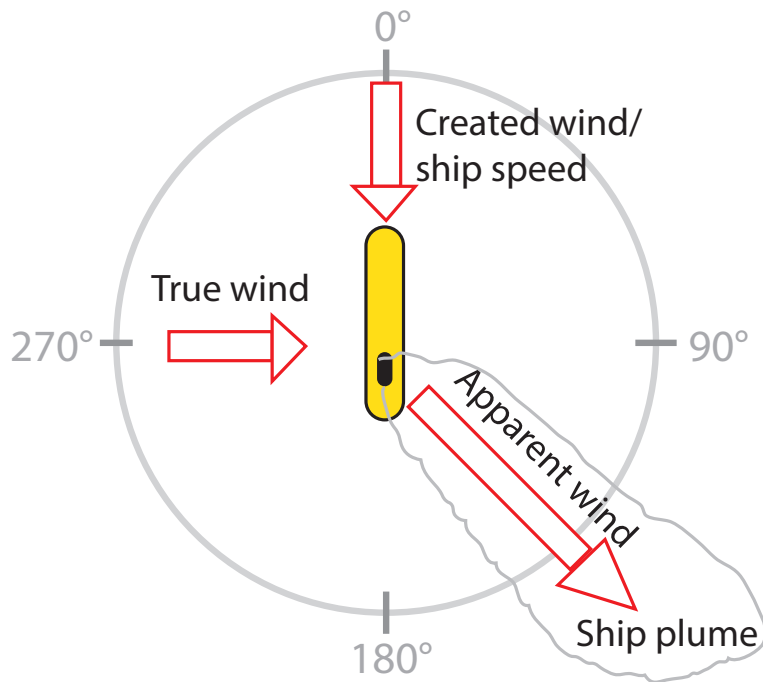


Fig. 2. The apparent wind is the resulting wind from the created wind from the speed of the boat and the true wind. The ship exhaust plume follows the apparent wind (from Berg et al., 2012).

Field test of available methods to measure remotely SO_x and NO_x

J. M. Balzani Lööv et al.

Title Page	
Abstract	Introduction
Conclusions	References
Tables	Figures
◀	▶
◀	▶
Back	Close
Full Screen / Esc	
Printer-friendly Version	
Interactive Discussion	

Field test of available methods to measure remotely SO_x and NO_x

J. M. Balzani Lööv et al.

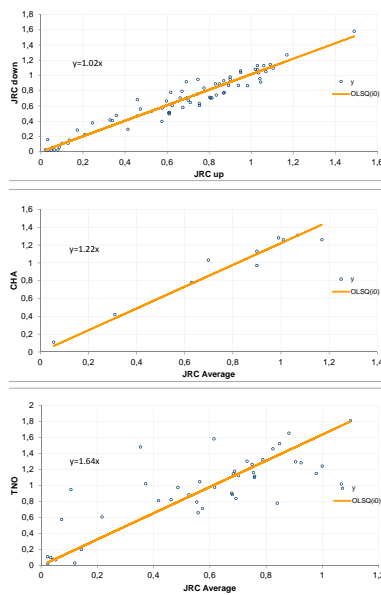
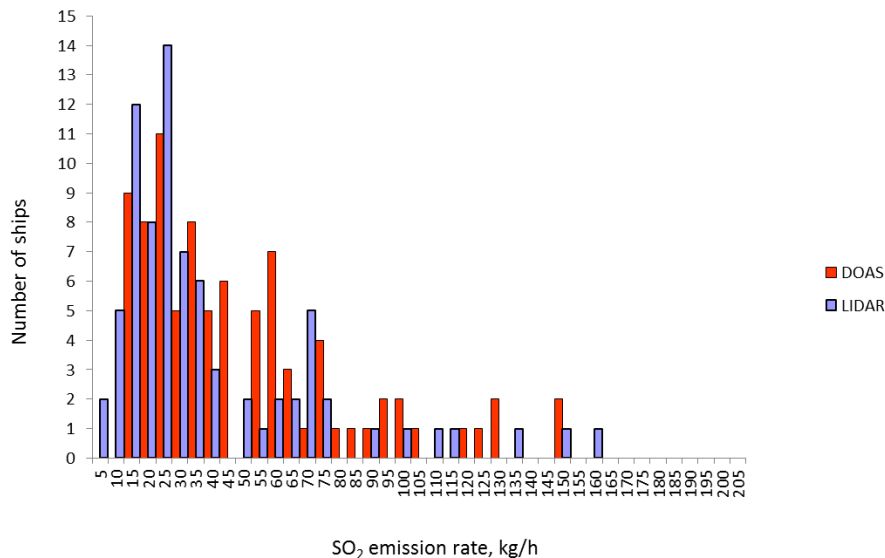


Fig. 4. Comparison of FSC, expressed in percent sulphur by mass in fuel, determined by “sniffer” measurements (see text). “JRC up” and “JRC down” are the two JRC sampling points, “JRC Average” is the average of these two points. “CHA” and “TNO” are the measurements performed at the same time on the same ship. Regression lines, forced through (0,0), have been obtained by orthogonal regressions. The number of outliers removed is 3 in the upper figure, 1 in the middle figure, and 2 in the lower figure.

[Title Page](#)
[Abstract](#)
[Introduction](#)
[Conclusions](#)
[References](#)
[Tables](#)
[Figures](#)
[Back](#)
[Close](#)
[Full Screen / Esc](#)
[Printer-friendly Version](#)
[Interactive Discussion](#)

Field test of available methods to measure remotely SO_x and NO_x

J. M. Balzani Lööv et al.

**Fig. 7.** SO₂ emission rate distribution as measured by the LIDAR and by the DOAS techniques.

Field test of available methods to measure remotely SO_x and NO_x

J. M. Balzani Lööv et al.

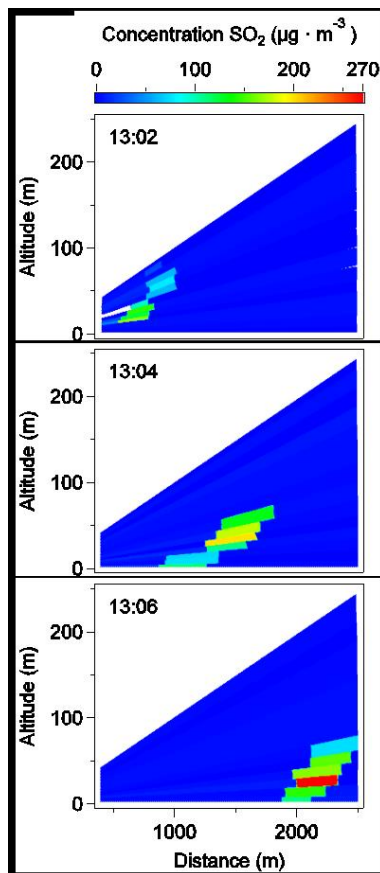


Fig. 8. Three sequential LIDAR measurements during the departure of Stena Hollandica on 17 September 2009. The blue area is the area covered by the LIDAR scans.

[Title Page](#)[Abstract](#)[Introduction](#)[Conclusions](#)[References](#)[Tables](#)[Figures](#)[◀](#)[▶](#)[◀](#)[▶](#)[Back](#)[Close](#)[Full Screen / Esc](#)[Printer-friendly Version](#)[Interactive Discussion](#)

Field test of available methods to measure remotely SO_x and NO_x

J. M. Balzani Lööv et al.

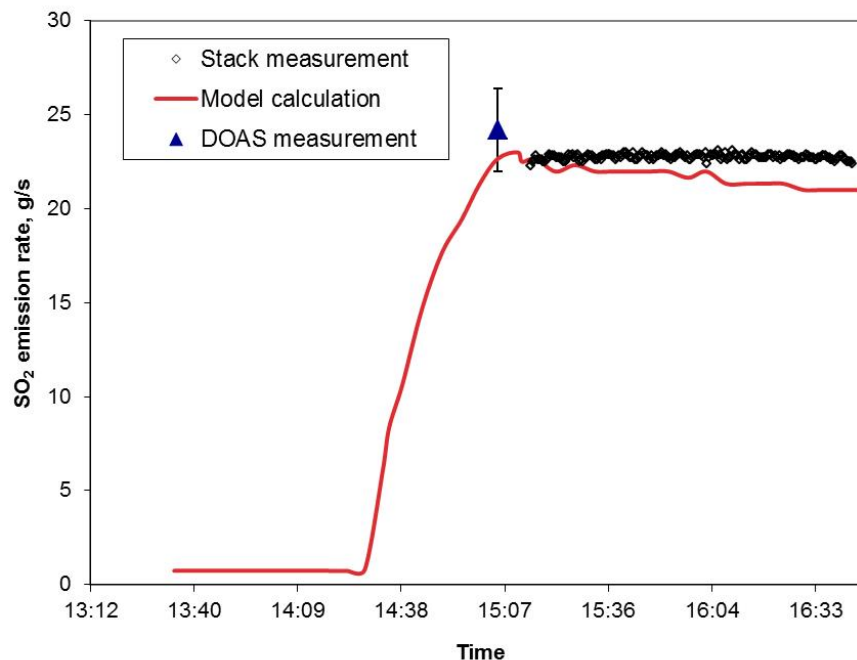


Fig. 10. Comparison of 7 repeated UV-DOAS measurements of Stena Hollandica (blue triangle, mean and standard deviation) performed by helicopter on 25 September 2009, with on-board stack measurements results (black diamonds). The corresponding model simulation is also indicated (red line).

Field test of available methods to measure remotely SO_x and NO_x

J. M. Balzani Lööv et al.

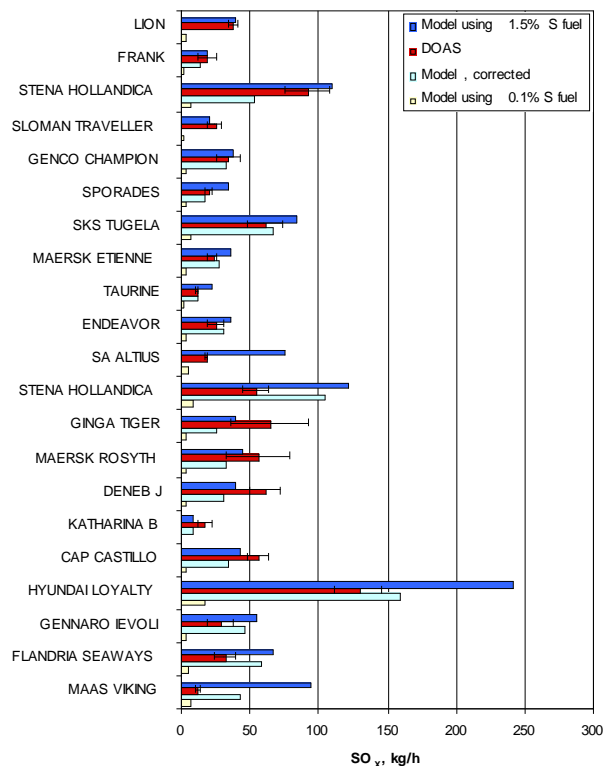


Fig. 11. Comparison of DOAS measurements performed by helicopter (in red), the modelled SO_x emission from the targeted vessel (assuming 1.5% (m/m) fuel sulphur ratio for main engines and 0.5% (m/m) for auxiliaries, in blue), the modelled emissions corrected with the sniffing measurement (taken sulphur ratio determined by sniffing), and the model results for a future scenario where ships run with 0.1% (m/m) sulphur fuel.